



ARAB REPUBLIC OF EGYPT
ATOMIC ENERGY ESTABLISHMENT
DEPARTMENT OF METALLURGY

SIZE AND SURFACE AREA ANALYSIS
OF SOME METALLIC AND
INTERMETALLIC POWDERS

M.A.A. EL
A

EL-SAYED
DIR.

NUCLEAR ENGINEERING
ATOMIC ENERGY ESTABLISHMENT

DEPARTMENT OF METALLURGY
CAIRO, A.S.

CAIRO, A.S.

AREABE / Rep. 305

We regret that some of the pages in the microfiche copy of this report may not be up to the proper legibility standards, even though the best possible copy was used for preparing the master fiche

AREAE/Rep.-305

ARAB REPUBLIC OF EGYPT
ATOMIC ENERGY ESTABLISHMENT
DEPARTMENT OF METALLURGY

SIZE AND SURFACE AREA ANALYSIS
OF SOME METALLIC AND
INTERMETALLIC POWDERS

BY

M.A.A. El-Masry, A.A.El-Sayed
AND M.F. ABADIR.

1988
NUCLEAR INFORMATION DEPARTMENT
ATOMIC ENERGY POST OFFICE
CAIRO, A.R.E.

CONTENTS

| | Page |
|--|------|
| ABSTRACT..... | i |
| NOMENCLATURE..... | 1 |
| INTRODUCTION..... | 2 |
| EXPERIMENTAL TECHNIQUES AND EQUIPMENT..... | 3 |
| EXPERIMENTAL RESULTS..... | 4 |
| REFERENCES..... | 18 |
| DISCUSSION AND CONCLUSION..... | 8 |

ABSTRACT

The powder characterization of three intermetallic compounds (CrB, B₄C and Si₃N₄) and three metallic powders (Fe, Co, and Ni) has been performed. This included the determination of powder density, chemical analysis, impurity analysis, shape factor, particle size analysis and specific surface area.

The particle size analysis for the six powders was carried out using three techniques, namely; the Q-23, the Microtrac and the Fisher Subsieve and Sizer. It was found that the analysis of the two powders deviates from the log-normal probability distribution and the deviation was corrected.

The specific surface area of the powders was measured using the high speed surface area analyser (BET method), and it was also calculated from surface area analysis findings. The BET technique was found to give the highest specific surface area values, and this was attributed to the inclusion of internal porosity in the measurement.

INTRODUCTION

The use of materials in finely divided forms is very common and diverse. Particle size distribution is one of most basic physical properties of powders and it affects in turn their physical and chemical characteristics as well as the properties of final products made from these powders.

Numerous techniques are utilized for determining particle size distribution. Each technique, however, has its own limitations and practically there is no general method that can be applied to all types of powders. The techniques are basically divided into direct and indirect methods. In the first category, size is directly obtained e.g. by sieve analysis, light and electron microscopy (1, 2-4). In the indirect technique, the effect of particle size on a certain property is measured and related to the size. This includes sedimentation (1,3-6), photo-effects (4,7), electrical effects (4,5,7-9), sonic analysis (9) radiation (7), X-ray analysis (7) and surface area methods (3,9-11).

Several investigators e.g. Cadle (1), Stokes (7) and Ferat (9) have established varying approaches to the definition of particle size, the most accepted of these being the projected area diameter. General presentation of the data on particle size either in histograms or cumulative curves are generally used (12,13).

Normally statistical laws are applied to the size distribution (2). The binomial distribution law applies when the number of particles is small. The normal distribution law is used when the 50% value of the oversize or undersize curve is equal to the arithmetic mean diameter. However, if the 50% value and the arithmetic mean value are not equal the log-normal probability distribution law or the abnormal-log normal laws are used.

In the present work six intermetallic and metallic powders are investigated, namely CrB, B_4C , SiB_4 , Fe, Co and Ni. These materials and their combinations enjoy both high hardness and erosion resistance and find wide applications in their pressed/sintered forms in nuclear, aerospace and other industries. Powder characterization including powder density, size analysis, surface area and chemical analysis were performed.

2. EXPERIMENTAL TECHNIQUES AND EQUIPMENT

2.1. Powder Density:

Powder density was determined by a null pycnometer, where the pressure change inside the cup of the pycnometer, due to the introduction of a certain mass of the powder, is used to calculate the real volume of the powder and hence its density. The equipment is normally calibrated each run.

2.2. Size Analysis:

Three techniques are used for size determination, namely the Microtrac, the Quantimet-23 and the Fisher Subsieve and Sizer. In the Microtrac method, the particle size is a function of the angle of the scattered light. Provision of a laser light source, appropriate filters and powerful microprocessors made the technique reliable and reproducible. The total range span of the microtrac analyser used is from 1.9 to 176 μm , divided into 13 channels of progressively greater width, so the percentage volume corresponding to each channel is obtained.

In the Q-23 method, the projected area diameter of the particle is determined as picture points and then converted into microns and placed in the appropriate size category of the minicomputer. The percent number corresponding to each category is then obtained.

The average shape factor $\left[\frac{\text{area}}{(\text{perimeter})^2} \right]$ is also obtained only for particles containing 25 picture points or more. As for particles containing less than this value, the shape factor will be in error as the perimeter value will be more than the area thereby producing a shape factor larger than that of a perfect circle.

The Fisher Subsieve and Sizer is based on the Kozney-Carman equation which relates the pressure drop of a permeating fluid due to its passage through a porous bed of the powder, to its average particle size, i.e. this is a single point technique.

2.3. Specific Surface Area Measurement:

It was measured using the high speed surface area analyzer model 2200. This technique is based on the BET theory i.e. the determination of the weight of nitrogen adsorbed to form a monolayer on the surface of the powder particles. By multiplication of the number of nitrogen molecules by the cross sectional area of a nitrogen molecule, the total surface area is obtained (14).

2.4. Chemical and Impurity Analysis:

The techniques and equipment used are given elsewhere (15).

3. EXPERIMENTAL RESULTS

3.1. Density, Impurity Content and Shape Factor for the Powders:

The density in g/cm^3 by the null pycnometer, the percent by weight impurity by the spark source mass spectrophotometry and shape factor together with the percent deviation from sphericity by the Q-23 are given in Table (1).

3.2. Particle Size Analysis:

3.2.1. chrome trioxide size analysis:

The particle size analysis by the Q-23 is shown in Fig.(1), as the percentage undersize (number) against the size in microns. the 50% value from this figure and the calculated arithmetic mean diameter are different. When the data were plotted on a log-normal probability paper a curve rather than a straight line was obtained Fig.(2).

Average diameters were calculated employing the Hatch-Choate transformation equations (6) and the linear regression straight line relationship of Fig. (2). The values are given in Table (2). In the same table, calculated average diameters from Q-23 results are given.

The size analysis for this powder by the use of the Microtrac is plotted on ordinary paper, Fig. (3) as the percent volume under-size. The log-normal probability plot for this powder, Fig (4) gives straight line relationship. Average Microtrac diameters are included in Table (2)

3.2.2. Silicon tetraboride size analysis:

The size analysis by the Q-23 is determined and a graph similar to Fig. (1) is obtained. Fig. (5) represents the log-normal probability plot and the curve is asymptotic towards the upper limit size. In this case $\left(\frac{d - d_0}{d_0 - d}\right)$ is plotted against (\emptyset) . A straight line is obtained and average diameters are calculated, Table (3). The Microtrac size analysis performed, has shown also that the distribution do not obey the normal probability distribution law. The plot of these results on a log-normal probability paper is given in Fig.(6). It is clear that the curve is asymptotic towards a small value which is not equal to zero, Therefore $(d-d_0)$ rather than (d) is plotted against (\emptyset) and a straight line is obtained from which the

various average diameters are derived also by direct calculations from the results of the Q-23 and given in Table(3)

3.2.3. boron carbide particle size analysis:

The log-normal probability plot for the Q-23 results is similar to Fig. (2) hence the normal procedure was followed to determine average diameters, Table (4). Microtrac results are almost similar to these of Q-23 and given in the same table.

3.2.4. cobalt powder size analysis:

The Q-23 findings showed that this powder has an abnormal log-normal probability distribution similar to SiB_4 results, Fig. (5). Q-23 and microtrac results which are almost similar, are presented, together directly calculated values in Table (5)

3.2.5. nickel powder size analysis:

The particle size analysis by the Q-23 had been executed and the average diameters are given in Table (6). The histogram of this distribution showed that the nickel powder has a four modal distribution which is totally different from the Microtrac results. Fig. (7) is the log-normal probability plot of the microtrac results. It is obvious that the curve has a point of inflection and the parent distribution curves intersect on the log-normal probability paper. The equation of this curve has been derived using the least square curve fitting technique, namely Gauss-Jordan elimination method (16). An equation of the third order is suitable in this case. the point of inflection is precisely determined and located as (F). The size frequency histogram Fig. (8) indicates that this powder has a bimodal distribution and that the two median values from this figure, d_1, d_2) are $13.8 \mu\text{m}$ and $105 \mu\text{m}$ respectively. d_1 and d_2 are located on the 50% probability and connected to the point of

inflection by straight lines. Since the point of inflection is common to both original distributions and since any of these distributions should appear as a straight line of the log-normal probability paper, it is sufficient to have two points for determining each distribution viz: the point of inflection and the median. The standard deviation for each distribution is calculated. The values of (f) , [fraction (f) , representing the first fraction of the powder], is then computed from the log-normal probability equation after integration for bimodally distributed powder. The integrated form of this equation is:

$$\Phi = 50 - 100f \operatorname{erf} \left[\frac{\ln d / \bar{d}_1}{\ln \sigma_1} \right] - 100(1-f) \operatorname{erf} \left[\frac{\ln d / \bar{d}_2}{\ln \sigma_2} \right].$$

where;

Φ is the percentage greater than a certain size, and (f) is the 1st fraction (f_1) and $\operatorname{erf} \left(\frac{\ln d / \bar{d}}{\ln \sigma} \right)$ is the error function, (obtained from tabulated figures, (17)). Since the experimental values of (Φ) are known, (f) can be calculated from the above equation. The calculated values of (f) are given in Table (7).

The first four calculated values of (f) and also the values corresponding to (75 μ m) are very close and seem to be independent of (Φ) . These values are averaged and the average is taken as the fraction (f_1). The calculated values of (f_1) and (f_2) are then used to calculate the values of (Φ) using the same integrated form of the log-normal probability distribution equation given before. The calculated values of (Φ) are given in Table (7). $(\Delta\Phi)$, which is difference between the measured and the calculated values of (Φ) are given also in the same table. The various average diameters are given in Table (6)

3.2.6. Iron powder size analysis:

The particle size analysis for this powder by the Q-23 showed that it does not obey the normal probability distribution law, so it may obey the log-normal probability distribution law or one of its modifications. The various averages are calculated and given in Table (8). The average diameters from the Q-23 and the log-normal probability distribution are not derived since the data points were not enough. The microtrac findings showed that this powder do not obey the normal probability distribution and a curve like that for nickel powder Fig. (7) and the frequency histogram for this powder showed that it has two modal distributions. The two medians are obtained from the figure, and the new distribution, as followed in case of Ni powder, is given in Table (8). Calculated average diameters are given in Table (9).

3.3. The Specific Surface Area:

The measured and the calculated values of the specific surface area in m^2/g are given in Table (10) for all powders used in this investigation.

4. DISCUSSION AND CONCLUSION

It is important in reviewing the size analysis data to know whether the particle amount is given in terms of number, mass, volume or surface of particles. This has an enormous bearing on the meaning of the graph. The method of sampling is also important. The sample must be representative for the powder. In other words the finite number of the particles in the sample should be representative for the infinite number of particles in the powder very well. It should also be made sure that the upper and the lower sizes of the powder are in the specified range of the equipment. Although the percent

oversize or undersize graphs are commonly used in the representation of the size analysis results it is much better to use the normal probability and log-normal probability graphs to know which of these distributions does the powder in question follow.

All powders investigated in this research obey the log-normal probability distribution law, Fig.(4) . Any deviation from the straight line relation may be attributed to one or more of the following reasons:

- a) The elimination of some of the coarse particles. This will give a curve which asymptotes toward the upper size, Fig. (5).
- b) Elimination of some of the fine particles and this will give a curve which asymptotes towards the lower size Fig(6)
- c) The elimination of some of the coarse and the fine particles simultaneously and this will give a curve which asymptotes to both the upper and the lower sizes, Fig (2).
- d) Bimodally distributed powders give curves with one point of inflection Fig. (7). The powders are the result of mixing powders from different sources or the limitations imposed on the growth during crystallization or the incomplete elimination of some fractions. In this case size frequency histogram, Fig. (8), is necessary to locate the value of the median diameters. It is obvious that the findings of the particle size analysis by the Q-23 and the microtrac that results are not identical. This is fairly expected and is basically due to the difference in the technique used. So it is important when reporting size analysis to define the technique and equipment used. An important result which worths mentioning here is that all the mean diameters obtained employing both techniques, lie between the geometric mean diameter by count (dgc) and weight mean diameter (dw).

The results of the surface area measurement and calculations show that the specific surface area determined by the nitrogen adsorption, (BET), has the highest value and those calculated from the particle size analysis are the lowest. The Fisher Subsieve and Sizer gave values in between.

The highest values obtained by the use of the ^{ah} high speed surface area analyzer, (BET) is due to the fact that both the external and the internal surface areas are taken into consideration. The nitrogen molecule may be fixed in the small microcracks (6), microfissures, the very small pits and the surface pores. This will give rise to an increase in the specific surface area due to the increased amount of nitrogen adsorbed. Another reason that should be mentioned here is the fact that a deviation from the monolayer may occur at the edges of the particles and more than one molecular layer is accumulated giving rise to an increase in the volume of the nitrogen and leading to an increase in the specific surface area. Similar observations were reported elsewhere (14).

The medium values obtained from the Fisher Subsieve and Sizer indicate that some of the internal surface area was accessible by the fluid, (air in this case), and this led to the specified values.

The specific surface areas calculated from the size analysis have the lowest values because only the external surface areas have been taken into consideration.

Unfortunately, to the knowledge of the authors no mathematical relation has been found to relate the external to the internal surface areas. It is essential here then to define techniques and equipment used when reporting surface area measurement.

Table (1)
Density, impurity, shape factor, percent deviation from sphericity and oxygen content.

| Powder | Density | % Impurity | Character | | |
|-------------------------|---------|------------|--------------|----------------------------|------------------------|
| | | | Shape factor | %Deviation from sphericity | O ₂ Content |
| Chromic Oxide Cr/B 1.33 | 5.059 | 10.4 | 0.056 | 29.9 | 2.66 |
| Silicon tetra- boride | 2.48 | 0.486 | 0.062 | 21.5 | 5.15 |
| Boron Carbide | 2.3172 | 3.9095 | 0.061 | 23.9 | 0 |
| Cobalt | 8.22 | 4.9056 | 0.045 | 43.3 | 0.56 |
| Nickel | 8.8355 | 1.53 | 0.059 | 26 | 0.094 |
| Iron | 7.7265 | 0.2875 | 0.053 | 27 | 1.1 |

Table (2)
Average diameters for CrB by different techniques " μ m"

| Symbol | Technique | | |
|-----------------|-----------|-------------|-----------|
| | Q-23 | Calculation | Microtrac |
| d _{gc} | 6.3 | 10.9 | 6.9 |
| d _{ev} | 6.6 | 12.6 | 8.5 |
| d _g | 11.6 | 16.1 | 10.3 |
| d _v | 15.5 | 19.4 | 12.6 |
| d _{vs} | 27.7 | 28.4 | 18.7 |
| d _{gb} | 37.1 | 35.9 | 22.8 |
| d _w | 49.2 | 60.7 | 27.8 |

Table (3)
Average Diameters For SiB₄ by Different
Techniques "μm"

| Symbol | Technique | | |
|-----------------|-----------|-----------|--------------|
| | Q-23 | Microtrac | Calculations |
| d _{gc} | 1.46 | 1.13 | 1.64 |
| d _{av} | 1.19 | 1.24 | 2.14 |
| d _s | 3.29 | 1.37 | 2.6 |
| d _v | 4.92 | 1.5 | 3.01 |
| d _{vs} | 11.07 | 1.82 | 4.06 |
| d _{gm} | 16.6 | 2 | 5.19 |
| d _w | 24.58 | 2.2 | 4.84 |

Table (4)
Average Diameters for B₄C by
Various techniques "μm"

| Symbol | Technique | | |
|-----------------|-----------|-----------|--------------|
| | Q-23 | Microtrac | Calculations |
| d _{gc} | 1.4 | 0.93 | 2 |
| d _{av} | 1.6 | 1.15 | 2.2 |
| d _s | 1.9 | 1.43 | 2.5 |
| d _v | 2.3 | 1.78 | 2.8 |
| d _{vs} | 3.2 | 2.75 | 3.6 |
| d _{gm} | 3.8 | 3.42 | 5.4 |
| d _w | 4.4 | 4.25 | 4.9 |

Table (5)
Average Diameters for Co by
Various Techniques " μm "

| Symbol | Technique | | |
|----------|-----------|-----------|--------------|
| | Q-23 | Mictotrac | Calculations |
| d_{gc} | 10.2 | 3.8 | 10.6 |
| d_{av} | 13.9 | 5 | 12.5 |
| d_s | 19.1 | 6.4 | 14.1 |
| d_v | 26.2 | 8.3 | 15.7 |
| d_{vs} | 49.3 | 13.9 | 19.5 |
| d_{gm} | 67.8 | 17.9 | 49.5 |
| d_w | 91.7 | 23.1 | 23.0 |

Table (6)
Average Diameters for Nickel By
Different Techniques, " μm "

| Symbol | Technique | |
|----------|--------------|-----------|
| | Calculations | Microtrac |
| d_{gm} | 134.7 | 103.0 |
| d_{gc} | 77 | 8.1 |
| d_{av} | 80.5 | 12.3 |
| d_s | 82.3 | 18.9 |
| d_v | 83.4 | 28.8 |
| d_{vs} | 85.7 | 67.4 |
| d_w | 89.8 | 157.4 |

Table (7)
Heterogeneous distribution for nickel
powder by the microtrac.....

| ^d microns | Ø _{measured} | f | Ø _{calculated} | ΔØ |
|-------------------------|-----------------------|-----------|-------------------------|----------|
| 1.4 | 99.9 | --- | --- | --- |
| 3.35 | 99.375 | 0.0257 | 99.3034 | 0.0716 |
| 4.7 | 99.075 | 0.03074 | 99.1336 | -0.0586 |
| 6.65 | 98.8 | 0.03069 | 98.8696 | -0.0696 |
| 9.4 | 98.475 | 0.027869 | 98.4376 | 0.0374 |
| 13.5 | 98.225 | 0.0147 | 97.4645 | 0.7305 |
| 19.0 | 97.15 | 0.002 | 94.5604 | 2.5896 |
| 26.5 | 96.625 | 0.046598 | 92.2834 | 4.3416 |
| 37.5 | 94.875 | 0.1323165 | 86.0357 | 8.8393 |
| 54.0 | 89.875 | 0.233165 | 75.7844 | 14.0806 |
| 75.0 | 63.875 | 0.02784 | 63.8331 | 0.0419 |
| 106.5 | 21.4 | 0.38046 | 48.9716 | -27.5716 |
| 120.0 | --- | --- | 43.524 | --- |

Table (8)
Heterogeneous Distribution for the iron
powder by the microtrac.....

| d(μ m) | ϕ measured | f Calculated | ϕ Calculated | $\Delta \phi$ |
|-------------|--------------------|-----------------|----------------------|---------------|
| 1.4 | 98.7 | 0.4375 | 98.675 | 0.025 |
| 2.35 | 96.2 | 0.8675 | 94.725 | 1.475 |
| 4.7 | 93.0 | ----- | 91.322 | 1.678 |
| 6.65 | 89.1 | ---- | 86.049 | 3.051 |
| 9.4 | 83.5 | 0.8592 | 74.249 | 9.251 |
| 13.5 | 74.4 | 0.0873 | 69.547 | 4.853 |
| 19.0 | 60.6 | 0.3489 | 59.393 | 1.207 |
| 26.5 | 47.9 | 0.4828 | 49.238 | -1.338 |
| 37.5 | 29.2 | 0.7873 | 38.925 | -9.623 |
| 53.0 | 10.9 | -- | 29.749 | -18.849 |
| 75.0 | 5.8 | -- | 22.415 | -16.615 |
| 106.5 | 3.2 | -- | 16.858 | -13.158 |

TABLE (9)
Average Diameters for iron Powders using
Various techniques.

| Symbol | Technique | |
|----------|--------------|-----------|
| | Calculations | Microtrac |
| d_{gc} | 3.4 | 0.2 |
| d_{av} | 3.8 | 0.5 |
| d_s | 9.4 | 1.1 |
| d_v | 16.6 | 2.4 |
| d_{vs} | 52.1 | 12 |
| d_{gm} | 31.6 | 25.5 |
| d_w | 70.1 | 58.8 |

Table (10)
Specific Surface area m^2/g

| Technique Powder | Measured BET | Calculated Fisher | Q-23 | | Microtrac | |
|------------------|--------------|-------------------|------------|------------------------------------|------------|------------------------------------|
| | | | Calculated | Calculated from log-N Distribution | Calculated | Calculated from log-N Distribution |
| CrB | 3.08 | 0.16 | 0.42 | 0.042 | 0.07 | 0.052 |
| B ₄ C | 7.55 | 0.97 | 0.69 | 0.8 | 0.66 | 0.92 |
| SiB ₄ | 3.87 | 1.42 | 0.6 | D.22 | 0.55 | 1.33 |
| Co | 1.2 | 0.17 | 0.04 | 0.015 | 0.056 | 0.053 |
| Ni | 0.5 | | 0.0062 | | 0.01034 | 0.01043 |
| Fe | 1.2218 | 0.194 | 0.145 | | 0.047 | 0.065 |

REFERENCES

- (1) R.D. Cadle, "Particle size determination", Interscience Publishers, Inc. (1965).
- (2) Riyad Irani and Clayton F. Callis, "Particle size measurement, interpolation and application, John Wiley & Sons, (1966).
- (3) Symposium on the New Methods for Particle Size Determination in the Subsieve Range, (ASTM), (March 1941).
- (4) John D. Stockham and Edward G. Fochtham, "Particle Size Analysis" Ann. Arbor Science Publishers Inc., (1966).
- (5) The Society for Analytical Chemistry, "Particle Size Analysis" England, (1966).
- (6) H.E. Rose, "The measurement of particle size in very fine powders", Constable & Comany Ltd., (1950).
- (7) Ing. Zdenek, K. Jelinek, C. Sc. Organic Synthesis Research Institute, Pardubice, Czechoslovakia. "Particle size analysis", John Wiley & Sons, (1966).
- (8) Henry H. Hausner, "Modern Developments in Powder Metallurgy" vol. 1, Plenum Press, (1966).
- (9) Clyde Orr., Jr., J.M. Davalle, "Fine Particle Measurement, size, surface and pore volume" MacMillan Co., N.Y. (1960).
- (10) "Ultrafine Grain Ceramics", John J. Burke, McGraw Hill, (1966).
- (11) Sheppard et al. and Gadumm. Nature, 156, 463 (1975).
- (12) Richard D. Cadle, "Particle size, theory and industrial applications", Reinhold Publishing Corporation, (1978).

- (13) Frances Clark, "Advanced techniques in powder metallurgy"
McGraw Hill, (1968).
- (14) S. Lowel and J.E. Shields, Chapman Hall, N.Y. (1984).
- (15) M.A.A. El-Masry, "Ph.D. Thesis, Cairo Univ., (1983).
- (16) Richard Bellman, "Introduction to matrix analysis",
McGraw Hill, (1970).
- (17) Boris Parl, "Basic Statistics", Double Day and Co.,
Inc. Garden City, N.Y.

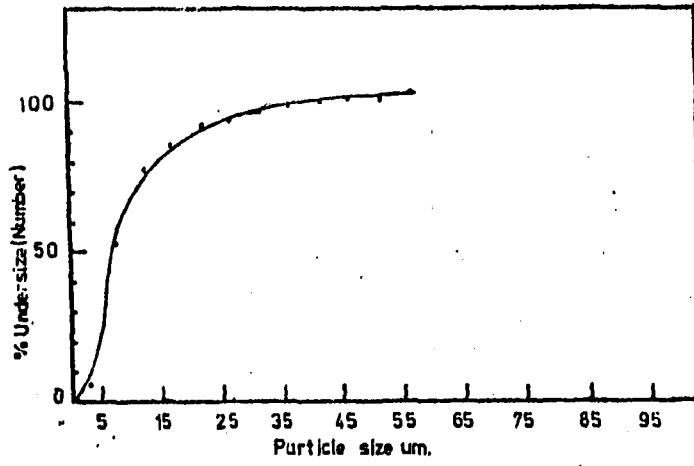


Fig.1 Particle size analysis for CrB by the Q-23.

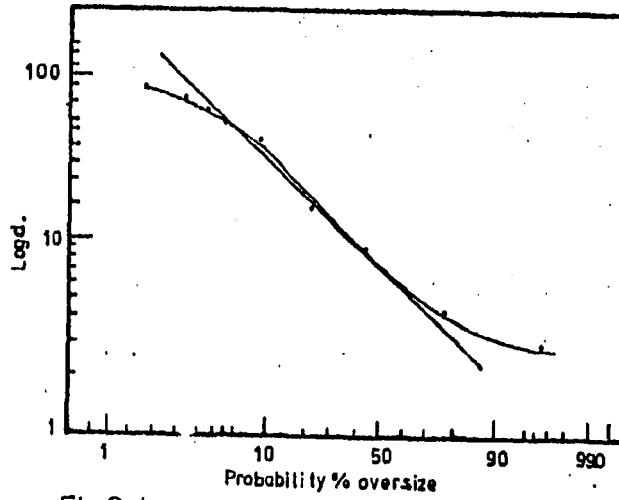


Fig.2 Log normal probability distribution for CrB by the Q-23.

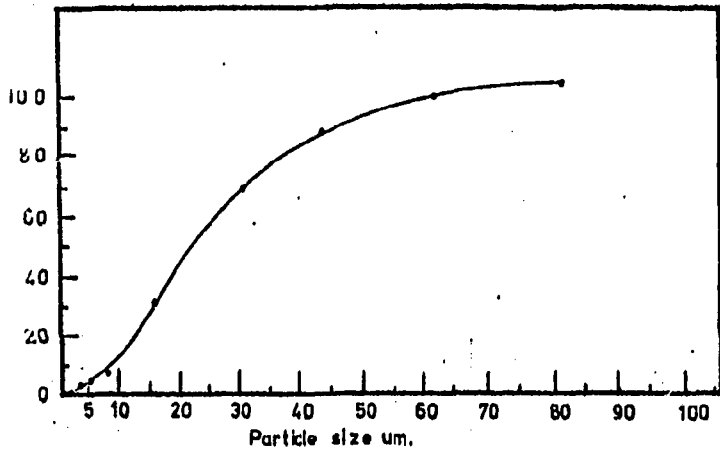


Fig.3 Particle size analysis for CrB by the microtrac.

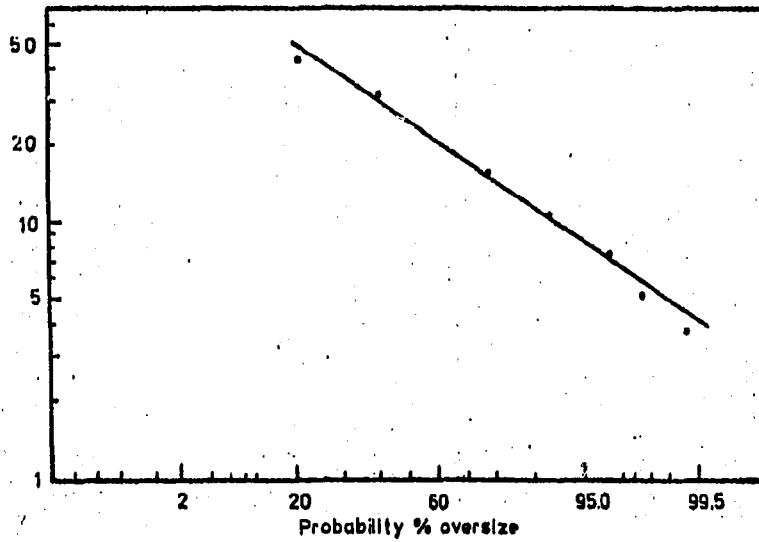


Fig.4 Log normal probability distribution for CrB by the microtrac.

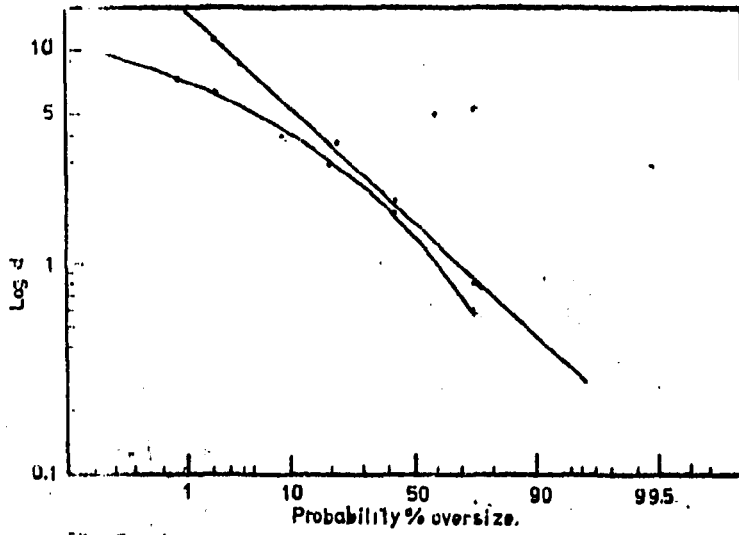


Fig.5 Log normal probability distribution for siB_4 by the Q-23.

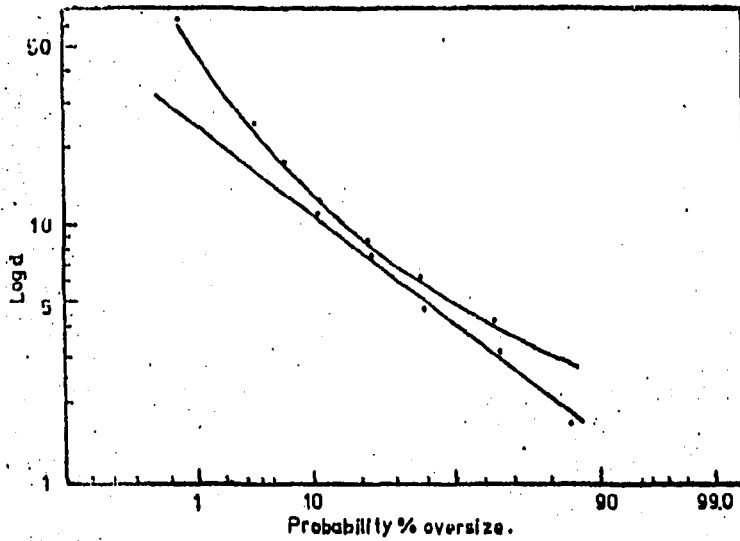


Fig.6 Log normal probability distribution for siB_4 by the microtrac.

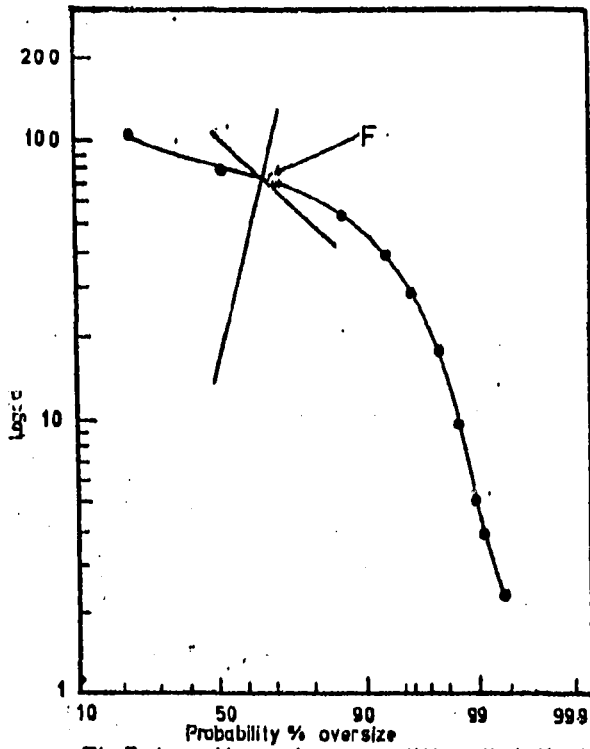


Fig.7 Log-Normal probability distribution for Ni by the microtrac.

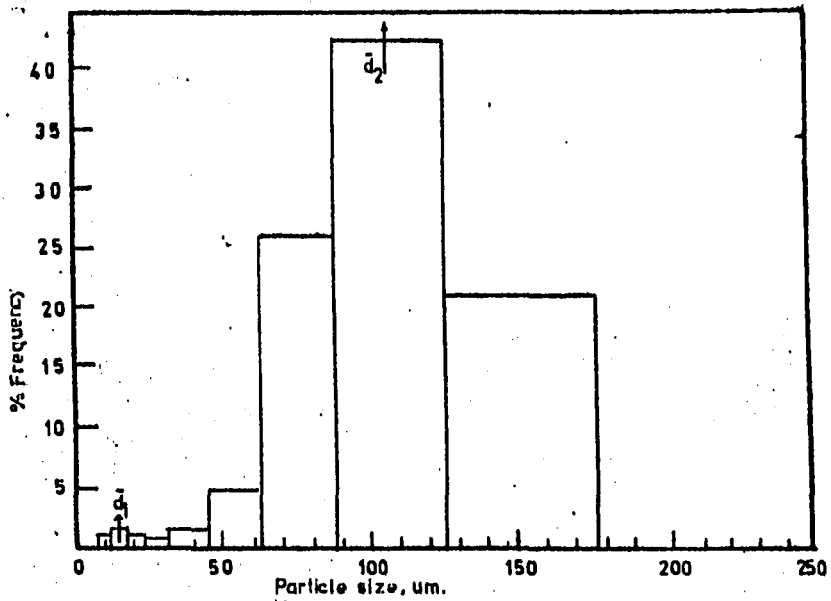


Fig.8 Frequency histogram for Ni by the microtrac.

NOMENCLATURE

- d_{gc} : The geometric median diameter by count.
- d_{av} : The arithmetic mean diameter.
- d_s : The surface mean diameter.
- d_{vs} : The volume surface mean diameter.
- d_v : The volume mean diameter.
- d_w : The weight mean diameter.
- d_{gm} : The geometric median diameter by weight
- ρ : The percent over a certain size.
- d_{∞} : The maximum diameter which the distribution asymptotes to.
- d_0 : The minimum diameter which the distribution asymptotes to.
- d : The median value on the size frequency histogram.
- σ : The standard deviation, the 50 percent value divided by the 84.13 value.